Simulation of running crowd dynamics: potential-based cellular automata model

Tao Yu[1,2], Hai-Dong Yang[1]

1College of Computer Science, Inner Mongolia University, Hohhot 010021, China
2Department of International Education, Hohhot Vocational College, Hohhot 010070, China

Corresponding author: Tao Yu (e-mail: yutaoqq@ 126.com).

ABSTRACT Running is often accompanied by fear or panic during emergency evacuation, and the evacuation of pedestrian crowds at different speeds poses additional challenges in terms of modeling and simulation. To investigate the fundamental interference of running pedestrians in the evacuation process, in this study, an extended cellular automata model was developed to simulate the evacuation of mixed groups of walking and running pedestrians in an area with multiple exits. The innovations of this extended model are the application of the dynamic potential field algorithm considering panic propagation, pedestrian running caused by panic, and pedestrian ratio and obstacle layouts. Running pedestrians, converted from walking pedestrians, were recognized by the number of k-nearest neighbors in the moving direction based on the Manhattan distance method. The effects of initial pedestrian density and obstacle layout were studied using numerical simulations. The simulation results indicate that a certain number of running pedestrians are needed to improve the evacuation efficiency, and the panic is contagious to others in that walking pedestrians transform into running pedestrians to accelerate the evacuation speed. The research provides insights for improving pedestrian-evacuation efficiency in facilities similar to the scene used in the experiment.

INDEX TERMS Running pedestrian flow, Cellular automata model, Pedestrian conversion, K-Nearest neighbors method, dynamic potential field

I. INTRODUCTION

With an increase in the occurrence of crowd accidents, research on emergency evacuation has gradually increased in recent years [1], [2]. A stampede in Seoul's Itaewon on Oct. 30, 2022, caused 158 deaths, and 196 injuries. More than two thousand pilgrims dead when a terrible stampede occurred in Mina, Saudi Arabia during Hajj 2015 [3]. Ten people died during the Astro World Musical Festival stampede in Houston, US State Texas on Nov 5, 2021. Traffic jams and stampedes are always accompanied by running, panic, push and trample et al., and without meaningful transmission management measures will led to these disasters. All inestimable losses in most accidents caused by crowds ' irrational behavior have posed challenges for urban planners and administrators. Understanding the internal mechanisms of pedestrian behaviors can help improving the safety and predicting the collection and evacuation behavior of pedestrians in complex scenes.

Running is a common behavior that always occurs in pedestrian emergency evacuations. Compared to walking, running exhibits more complex interactions between pedestrians; therefore, it is difficult to study. To investigate the evacuation dynamics of pedestrians with higher velocities, microscopic models were used to quantitatively predict the human movements. With the distinct advantages of efficiency, powerful scalability, and simple implementation, the cellular automata (CA) model has become one of the most widely used models for pedestrian evacuation. Zhou et al. [4] presented a multithreading mechanism for simulating pedestrian walking at different speeds. Kirchner et al. [5] used an extended cellular automata model to reflect the effect of increased maximal walking speed and reduced cell size on

pedestrian motion. Weng et al. [6] reproduced several typical pedestrian evacuation phenomena with different desired walking velocities by using a discrete small-grid analysis model. Yuan et al. [7] proposed a cellular automata model simulating pedestrian evacuation from a smoke-filled room based on two algorithms that modeled crowd behavior with different movement velocities. These studies provide effective methods for studying pedestrian evacuation at different speeds. However, high density pedestrians in emergency situations always suddenly accelerate, this sudden change in speed caused by panic and the characteristic of accelerating crowds is relatively rare in existing research. Therefore, this article aims to fill in the research gap of pedestrian evacuation with differentiated speeds.

The concept of potential used in cellular automata model can reflect the effect of route distance, pedestrian congestion, and route capacity to calculate the transition probability at every time step. Guo et al.[8], [9]proposed a generalized potential considering the number of front pedestrians on the target routes, which implies that route selection for target exits is determined not only by route distance but also by congestion. Xu and Huang [10] used a directional visual field to describe the prediction of pedestrian propagation and considered the partial free spaces near exits and pedestrians. However, these models neglect the effects of additional free spaces and obstacles; thus, the competition mechanism between pedestrians for free space also needs to be further explored.

Different behaviors may be triggered in emergencies, and the spread of fear has been observed in many video recordings from emergency situations. Minh et al. [11] stressed that emotions, such as fear and panic, play a significant role in pedestrian evacuation. Zhao et al. [12] used a susceptible-infected-Recovered-Susceptible (SIRS) model. Cornes et al. [13] defined a contagion radius area to determine the inner stress increment of a pedestrian surrounded by neighbors with different anxiety states. Fu et al. [14] used a multigrid model associated with abnormal emotion propagation to simulate counter-flow dynamics. Emotional contagion has been demonstrated in many cases; however, it is difficult to quantify and reproduce the influence of emotional propagation using discrete models. Based on Guo's model, we propose a dynamic potential field model for pedestrian evacuation. The extended cellular automata model was applied to model the crowd dynamics of running flows evacuating in a closed space with multiple exits and reveal the effects of emotion propagation on evacuation. The simulation results show that evacuation times are sensitive to running behavior, but not to obstacles.

The remainder of this paper is organized as follows. The extended model is described in Section II. Numerical simulation studies and other analyses of the influential parameters are presented in Section III. Sections IV and V present the discussion and conclusions, respectively.

II. MODEL DESCRIPTION

The model was established on a grid lattice space with an extended Moore neighborhood, as shown in Figure 1. Each cell can be occupied by only one pedestrian, obstacle, or empty. The cell size was $0.4m \times 0.4m$ [4], which was matched with a common adult size. Pedestrians are divided into two types according to their moving speed: walking pedestrian and running pedestrian. Walking pedestrian p_{ii} in cell (i, j) can move one cell at a time step to any vacant cell of the eight adjacent neighbors shown in Figure 1 (a), and running pedestrian p_{ii} in cell (i, j) can move through two cells at one time step to eight extended neighbor cells, as shown in Figure 1 (b).

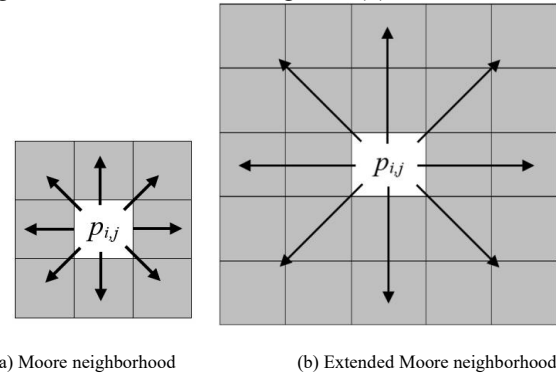(a) Moore neighborhood   (b) Extended Moore neighborhood

FIGURE 1. Transmission directions of walking and running pedestrians between cells.

Pedestrians move to a neighbor cell with a higher transition probability P_{ii}, the calculation formula of P_{ii} is shown in Eq. (1).

$$P_{ij} = N \cdot \exp(k_p p_{ij}) \exp(-k_D D_{ij})(1 - n_{ij}) \quad (1)$$

Where N is a normalization factor, p_{ii} is the static field, D_{ii} is the dynamic field, k_p and k_D are sensitivity parameters for scaling the static and dynamic fields, respectively, and n_{ii} is used to indicate whether a cell is vacant or occupied. $n_{ii} = 1$ if the cell is occupied by a pedestrian, obstacle, or wall; otherwise, $n_{ii} = 0$.

$$N = [\sum_{ij} \exp(k_p p_{ij}) \exp(-k_D D_{ij})(1 - n_{ij})]^{-1} \quad (2)$$

A. STATIC POTENTIAL FIELD

Static potential p_{ii} denotes the potential of cell (i, j), which indicates the distance from cell (i, j) to the exit. The algorithm for calculating the potential of cells is as follows[16].

Step 1. For each cell (i,j), if it is occupied by an obstacle or wall, set a fixed value of potential $p_{ii}=+\infty$. For each cell (i,j), if it is occupied by an exit, set the fixed value of potential $p_{ii}=0$.

Step 2. For each cell (i,j), if its neighboring cells are occupied by exits in the horizontal or vertical direction, set $p_{ii}=1$; the potential is fixed and added the cell to C_{check}, the set of cells that need to be checked. Set $\delta=0$.

Step 3. For each cell (i,j) in the set C_{check}, if $\delta \le p_{ii} \le \delta+1$, check all its neighboring cells (i_0,j_0), and then delete the cell (i,j) from the set C_{check}. If the potential of the cell (i_0,j_0) has not been determined, compute a temporary potential $\hat{p}_{i_0,j_0}$ regarding the subsequent four cases:

If cell (i_0,j_0) is unoccupied and positioned either horizontally or vertically, then

$$\hat{p}_{i_0,j_0} = p_{ij} + (1+c_{ij}) \tag{3}$$

If cell (i_0,j_0) is unoccupied and positioned either horizontally or vertically, then

$$\hat{p}_{i_0,j_0} = p_{ij} + (1+\alpha_o)(1+c_{ij}) \tag{4}$$

If cell (i_0,j_0) is unoccupied and located diagonally, then

$$\hat{p}_{i_0,j_0} = p_{ij} + (1+\alpha_d)(1+c_{ij}) \tag{5}$$

If cell (i_0,j_0) is unoccupied and located diagonally, then

$$\hat{p}_{i_0,j_0} = p_{ij} + (1+\alpha_d)(1+\alpha_o)(1+c_{ij}) \tag{6}$$

Step 4. For each cell, (i_0,j_0), assign its potential as the lowest value among all of its temporary potentials based on the temporary potential in Step 3, which is fixed and added to the set C_{check}.

Step 5. Set $\delta=\delta+1$; If all cells' potential have determined, then stop; otherwise, go to Step 3.

In this algorithm, three parameters are considered. The first intensity parameter c_{ii} is used to scale the impact of the route capacity on the potential. If cell (i,j) is situated within an aisle area that includes obstacles, then $c_{ii}=\bar{c}$ (>0); otherwise, $c_{ii}=0$. The second intensity parameter α_0 is used to adjust the impact of congestion on the potential, and $\alpha_0 \ge 0$. The third parameter α_d scales the rate at which the potential of neighboring cells increases in the diagonal direction, and we set $\alpha_d \in [0,1]$. The interval $[\delta,\delta+1]$ is confirmed for each iteration. Once the potential of a cell in the set C_{check} is in the interval, the potential values of all its neighboring cells are calculated. Thus, the potentials of all cells will be computed and fixed as δ increased. The potentials of cells in the area displayed in Figure 2, where the parameters are $\bar{c}=2$, $\alpha_0=2$, and $\alpha_d=\sqrt{2}-1$.

B. DYNAMIC POTENTIAL FIELD

Let D_{ii} denote the dynamic potential of cell (i,j), which is used to reflect the effects of route capacity, congestion degree, and pedestrian panic on transition probability. Owing to differences in gender, cognitive level, and psychological state, the route selection of pedestrians is different even when they are under the same conditions. Pedestrians always prefer maintaining a suitable distance to avoid interacting with others; thus, the free space ahead and congestion in adjacent cells make a significant contribution to route determination. However, pedestrians estimate the congestion based on the flow distribution in a larger range during the actual evacuation, and the considered direction is always forward, left, and right. Hence, we redefine the area of the dynamic potential field to enhance the effectiveness of the dynamic potential on the transition probability within the extended Moore neighbor.

Define D_{ii} as

$$D_{ij} = \alpha N_{neighb} - \beta N_{emp} \tag{7}$$

where N_{emp} represents the free space capacity, that is, the number of free cells in the moving direction. N_{neighb} represents the number of neighboring pedestrians in the extended Moore neighborhood, and α is the sensitivity parameter describing the effects of congestion on the dynamic potential and belongs to the interval $[0,1]$, β is a weighting factor for describing the route capacity and $\beta \in [0,1]$.

C. CONFLICT RESOLUTION MECHANISM

During the evacuation process, collisions occurred when the target cells of the two pedestrians were the same. In common cellular automata models, if conflicting pedestrian properties are the same, randomly selected a pedestrian to enter the cell. The difference in speed between walking and running pedestrians was significant, and the motion inertia was different. To solve pedestrian conflicts, we define J_{ii} as the competition probability for target cell (i,j),

$$J_{ij} = \frac{L_{ij}I_{ij}}{\sum_{i,j=1}^{n} L_{ij}I_{ij}} \tag{8}$$

where, L_{ij} is the distance from the pedestrian's current position to the exit, and I_{ii} is the number of steps taken by the pedestrian during continuous walking or running movements. According to the probability of competition, pedestrians with a high competition probability are given priority when entering. If the probability of competing target cells is the same, a pedestrian is randomly selected to enter the conflicting cell.

D. PEDESTRIAN ACCELERATION

Considering the panic contagion during emergencies, the presence of running pedestrians near walking pedestrians intensifies fear among walking pedestrians. If the number of running pedestrians in the neighborhood is greater than the number of walking pedestrians, the walking pedestrians will convert into running pedestrians and adhere to the rules of movement for running pedestrians. The k-nearest neighbor method based on the Manhattan distance was used to calculate the number of running pedestrians in the vicinity. In the region shown in Figure 2, the k-nearest neighbors of a cell (i, j) are searched, and if there are $n_p > k/2$ running pedestrians, the walking pedestrians in the cell (i, j) are converted into running pedestrians. Figure 2 illustrates the Manhattan distance for a neighborhood of 7×11 cell spaces, where the current pedestrian within the cell (i, j) is a walking pedestrian denoted as P_{walk}. Figure 2 shows the current distribution of pedestrians, if $k = 5$, there are three running pedestrians and two walking pedestrians within a range of three metric distances, $n_p = 3$, then the walking pedestrian within the cell (i, j) is converted into running pedestrian. If $k = 7$, there are three running pedestrians and four walking pedestrians within the nearest neighborhood of the cell, the conversion fails. Similarly, if $k = 9$, the conversion is successful and so on.
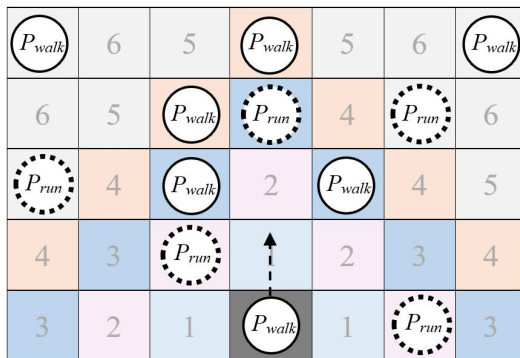

FIGURE 2. Pedestrians within the Manhattan distance

E. PEDESTRIAN UPDATE RULES

1. Set r as the initial proportion of pedestrians in the scene, where the proportions of walking and running pedestrians are p_{walk} and p_{run}, $p_{walk} + p_{run} = 1$, and the initial positions of the crowd are randomly distributed.

2. During evacuation, walking pedestrians search for nearest neighbors using the k-nearest neighbor method. If the number of running pedestrians is $n_p > k/2$, then walking pedestrians will converted into running pedestrians and follow the movement rules of running pedestrians. If this condition is not met, walking pedestrians move according to the original rules, moving one cell per time step. If there is a conflict, the competing probability is

calculated and one pedestrian is selected for enter. If there are no movable cells in the neighborhood, pedestrians stay and wait.

3. Running pedestrians follow the extended Moore neighborhood rules, moving two cells per time-step. If there is a conflict, one pedestrian is selected based on the competition probability. When there are no movable cells within the extended neighborhood, running pedestrians move according to the rules of walking pedestrians. If there are no movable cells in the neighborhood, pedestrians stay and wait.

4. When a pedestrian reaches the exit, it is considered a successful evacuation. When all the pedestrians have successfully evacuated, the evacuation is complete. The update rules for pedestrians are shown in Figure 3.
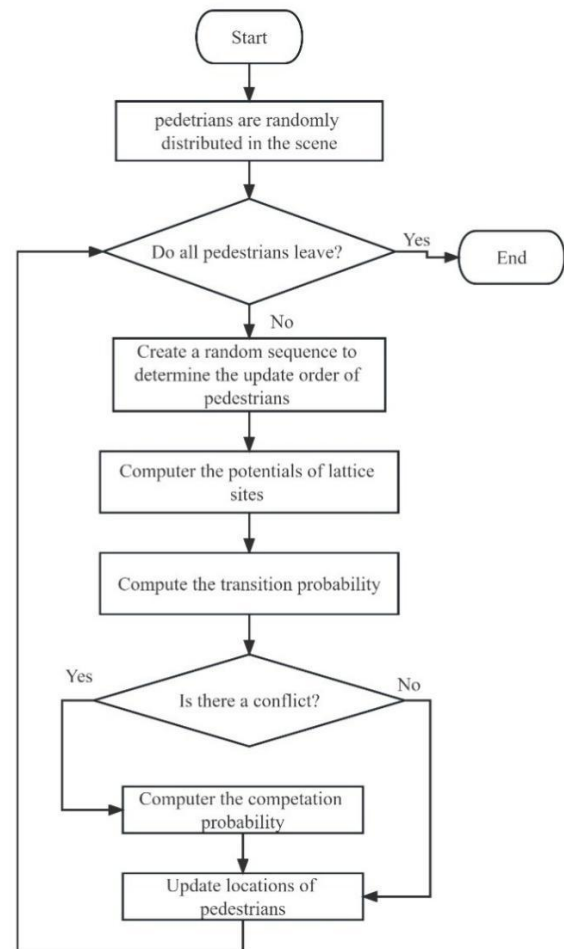

FIGURE 3. The flowchart of the model running.

III. NUMERICAL SIMULATION

A. SCENARIO DESCRIPTION
The extended model is applied to an indoor space, as shown in Figure 4. The size of the square room was

$24m \times 24m = 576m^2$, and the two exits were located symmetrically on the lower wall. The width of the exits was $4m$, and there was an $8m$ interval distance between these two exits.

The entire square region was discretized into 60×60 regular square cells, and each cell could accommodate one pedestrian. At the initial time of the simulation, N_p pedestrians randomly concluded that walking and running pedestrians were located in the region. The blue dots indicate walking pedestrians and the red dots indicate running pedestrians. The measurement area was used to measure the pedestrian density, pedestrian velocity, and flow at the steady stage. The size of the measurement area was $24m \times 8m$ and is next to the exits. Density ρ was defined as the ratio of the number of pedestrians to the number of cells in the measurement area. We define pedestrian velocity v as the ratio of the number of pedestrians adopting the forward direction to the total number of pedestrians in this measurement area [15], and flow as the number of pedestrians passing through the base line, that is, the number of pedestrians passing through the exits per second per meter ($peds / m \cdot s$).
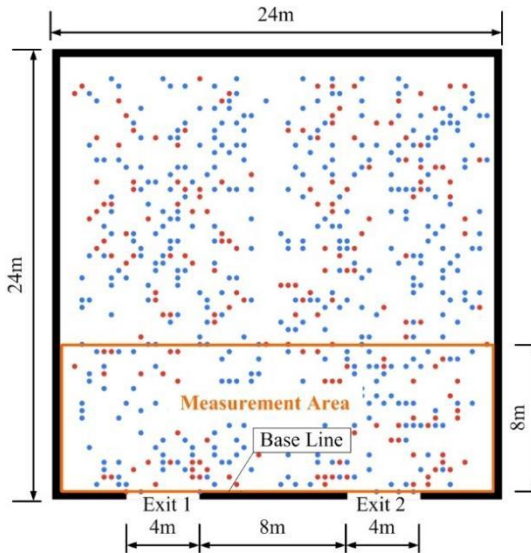
FIGURE 4. Simulation scenario.

B. THE IMPACT OF RUNNING PEDESTRIAN ON EVACUATION

The initial pedestrian ratio $r = N / Total\_Num$, N defined as the initial number of pedestrians in the room, and $Total\_Num$ is the total number of cells in the square space, i.e., 3600. The ratios of walking and running pedestrians were p_{walk} and p_{run}, and $p_{walk} + p_{run} = 1$.

As shown in Figure 5, the schema of pedestrian evacuation movements at time steps 10, 30 and 50 in the simulation presents the three stages of evacuation:

$p_{run} = 0.2$, $p_{run} = 0.6$, and $r = 0.2$. In the first stage (see Figure 5 (a) and (d)), all walking and running pedestrians were mixed and heading to the exits. In the second stage (see Figure 5 (b) and (e)), most running pedestrians surpassed walking pedestrians and concentrated near the exits. In the last stage (see Figure 5 (c) and (f)), most pedestrians left the room, while a few running people still jammed with other walking people, that is, running pedestrians had to move following the walking rules caused by limited space.
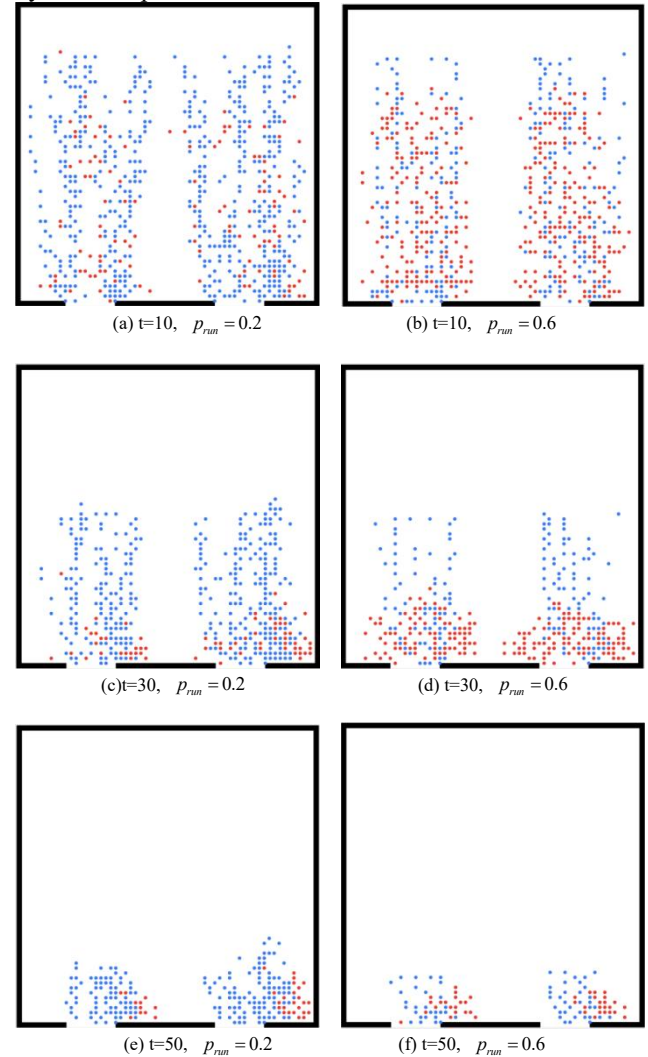
(a) t=10, $p_{run} = 0.2$ (b) t=10, $p_{run} = 0.6$

(c)t=30, $p_{run} = 0.2$ (d) t=30, $p_{run} = 0.6$

(e) t=50, $p_{run} = 0.2$ (f) t=50, $p_{run} = 0.6$

FIGURE 5. The schema of pedestrian evacuation movements with different ratios of running pedestrians at time steps 10,30 and 50.

It can be seen from Figure 5 that pedestrian evacuation when $p_{run} = 0.6$ is much faster than $p_{run} = 0.2$, which can be explained by the fact that in setting a fixed initial ratio of pedestrians, the more running pedestrians there, the faster the evacuation. Except when the initial ratio of pedestrians is low, the ratio of running pedestrians has little effect on evacuation time when $r = 0.2$ (see Figure 5 (a)), because the initial positions of pedestrians are located

randomly, running pedestrians can be evacuated in a very short time, and the minimum evacuation time is determined by the walking pedestrian farthest away from the exit.
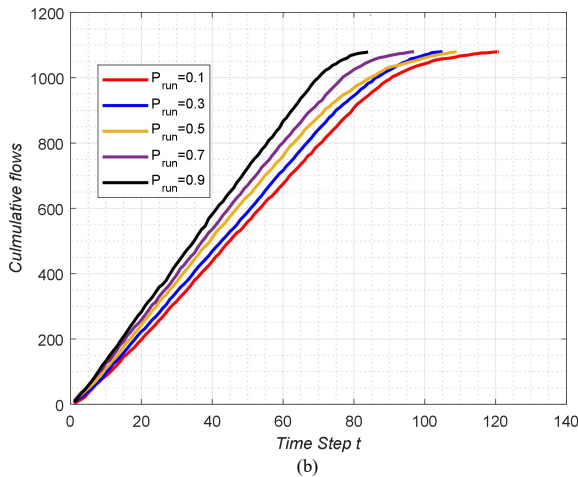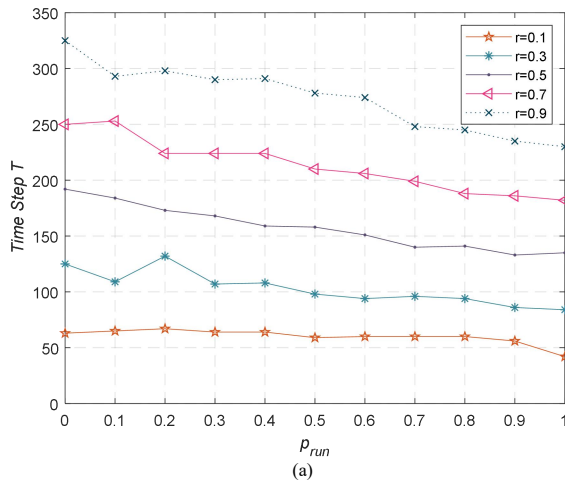

FIGURE 6. The relation of (a) evacuation time step against the ration of initial running pedestrians when $r = 0.1, 0.3, 0.5, 0.7, 0.9$, and (b) cumulative flows against time steps when $r = 0.3$ and $p_{run} = 0.1, 0.3, 0.5, 0.7, 0.9$.

To enhance the accuracy of the simulations, we calculated the average results of the 50 simulation runs. Figure 6 (a) shows the effect of the p_{run} on evacuation time steps when the ratio of initial pedestrians r varies from 0.1 to 0.9 with an interval of 0.2. As expected, a higher ratio of initial pedestrians resulted in longer evacuation times. The evacuation time is reduced with the increment in p_{run} when r is fixed, and the variation rate decreases when $p_{run} > 0.7$. This illustrates that running pedestrians showed a velocity advantage over walking pedestrians during the evacuation process, and the higher the density, the more obvious the advantage. As shown in Figure 6 (b), the cumulative flows increased with the evacuation time, and the evacuation time increased with a decrease in the running pedestrian ratio when the initial

pedestrian number was fixed. The greater the initial pedestrian density, the greater is the impact of the running pedestrian density on the evacuation time. Generally, running pedestrians is conducive to pedestrian evacuation.

As mentioned above, we assume that pedestrian walking and running at a fixed rate, and the free velocity of walking and running pedestrians are $1.56 m/s$ and $3.01 m/s$, respectively. According to the side length of a cell, each time step is approximately $0.4s$. The values of flow, velocity, and density were measured in the measurement area when pedestrians moved to a relatively stable station. Figure 7 presents a comparison of the velocity-density relation diagram when the proportion of running pedestrians is 0.1, 0.3, 0.5, 0.7, and 0.9. When the proportion of running pedestrians p_{run} is low, the velocity gradually decreases with an increase in density. When $p_{run} > 0.6$, the pedestrian velocity first increases to the maximum value, and then decreases rapidly, and the decreasing range becomes larger, which indicates that too many running pedestrians in high-density space cannot be evacuated effectively. Running pedestrians require more space to move; otherwise, they must move in a walking manner.
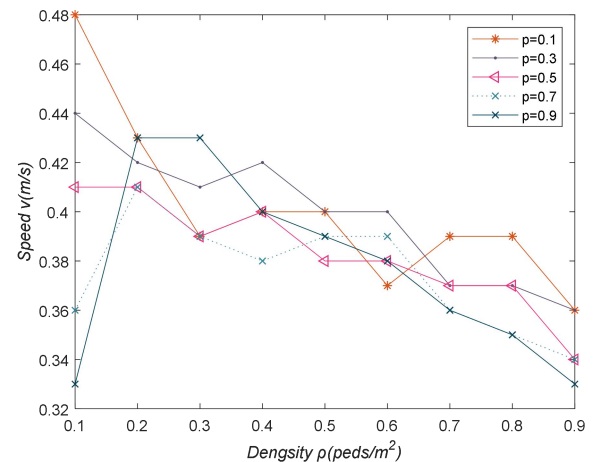

FIGURE 7. The relation of velocity against density.

In the evacuation process considering the running behavior, when the proportion of running pedestrians remains constant, the evacuation speed decreases as the density increases. When the proportion of running pedestrians is relatively high, in the early stages of evacuation, the overall speed increases because of the availability of space for running pedestrians to disperse. However, as pedestrians gathered towards the exit, the evacuation speed initially increased and then decreased as the density increased. Therefore, the curve in the graph shows that there is a noticeable promotion effect on

evacuation speed when pedestrian density increases slightly to $\rho = 0.2$ when $p_{run} = 0.7$ and $p_{run} = 0.9$.

C. THE IMPACT OF PANIC TRANSMISSION ON EVACUATION

In actual evacuation scenarios, particularly in emergency situations, pedestrian panic is easily transmitted to nearby pedestrians. When someone runs and overtook others, pedestrians affected by panic choose to accelerate. Pedestrians who are easily affected by emotions and moved with more running companies in neighborhoods are more likely to reach the conversion threshold.
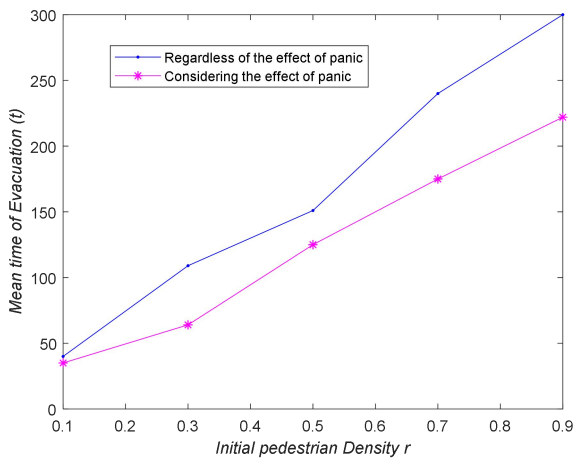

FIGURE 8. Mean time of evacuation of pedestrians against the initial pedestrian density when $p_{run} = 0.2$.

Without considering the pedestrian emotion influence parameter, pedestrian evacuation time increased with an increment of pedestrian density. As shown in Figure 8, when the density was high, the average evacuation time reached 300 time-steps. After considering the pedestrian emotion influence parameters, some walking pedestrians were converted into running pedestrians, which can significantly improve the overall evacuation efficiency. With an increase in pedestrian density, the growth rate of the average pedestrian evacuation time decrease. When the density is high, the average evacuation time is 222 time-steps; the higher the pedestrian density, the higher the proportion of walking pedestrians converted to running pedestrians, whereas the evacuation time was relatively reduced. The greater the pedestrian density, the higher the proportion of running pedestrians and the faster the transformation of pedestrian. However, when the pedestrian density is too high, there is almost no running space for running pedestrians, indicating that the impact of pedestrian density on evacuation efficiency is greater than the impact of the proportion of running pedestrians on evacuation efficiency.

The average number of pedestrians converted and the corresponding conversion time for each group of simulations were recorded. As shown in Table 1, when the proportion of running pedestrians is fixed, pedestrian density has the most significant influence of pedestrian conversion on the improvement of evacuation efficiency. We define the conversion rate as The ratio of converted pedestrians to the initial number of pedestrians.

TABLE 1
PEDESTRIAN CONVERSION RATE UNDER DIFFERENT INITIAL PEDESTRIAN DENSITIES AND RATIOS OF RUNNING PEDESTRIANS

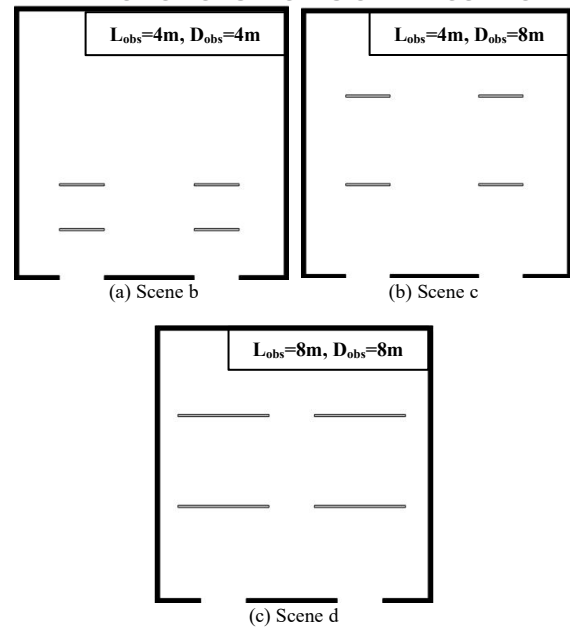|	ρ=0.1	ρ=0.3	ρ=0.5	ρ=0.7	ρ=0.9
$P_{run} = 0.1$	50.61%	96.60%	98.76%	98.80%	99.00%
$P_{run} = 0.3$	49.58%	94.17%	97.32%	98.27%	99.01%
$P_{run} = 0.5$	86.67%	99.26%	98.78%	99.20%	98.95%
$P_{run} = 0.7$	92.59%	99.07%	98.51%	99.20%	99.28%
$P_{run} = 0.9$	91.67%	99.07%	98.33%	98.81%	99.07%

D. THE IMPACT OF OBSTACLES ON EVACUATION

FIGURE 9. Scenarios with three different obstacle layouts.

Obstacles appear in most public places, and their location and size will affect pedestrian evacuation. A reasonable distribution of obstacles is necessary during an emergency evacuation. In this study, we investigated the effects of obstacles on evacuations. Compared to the original scene, there is little impact on pedestrian evacuation when the direction of the obstacle is perpendicular to the exit. Hence, three types of obstacle layouts were set up, and four obstacles with length of $4m$ or $8m$ and a width of $0.8m$ were distributed parallel to the exit. There were three scenes with different obstacle distributions, as shown in Figure 9. And distance from obstacles to exits are $4m$

and $8m$. The initial pedestrians were randomly distributed. The initial density of pedestrians is $r = 0.5$ and the proportion of running pedestrians is $p_{run} = 0.1$ in the simulation. The results are presented as the mean values of 20 runs.

Figure 10 shows a comparison of the pedestrian evacuation process in these three scenarios with the original scene a. The simulation results show that when the initial pedestrian density r is fixed, the larger the obstacle, the longer the time required for pedestrian evacuation. The change in location will also affect evacuation. The widths of the obstacles in scenarios b and c are the same as the exit width, and the overall evacuation is relatively slow compared with scenario a. The obstacles in scene d were relatively wider, the space gap for pedestrians to pass was very narrow, and the overall speed was significantly slower. In front of all obstacles, there is a triangular free space, which is a common self-organization behavior of pedestrians in a space with obstacles.
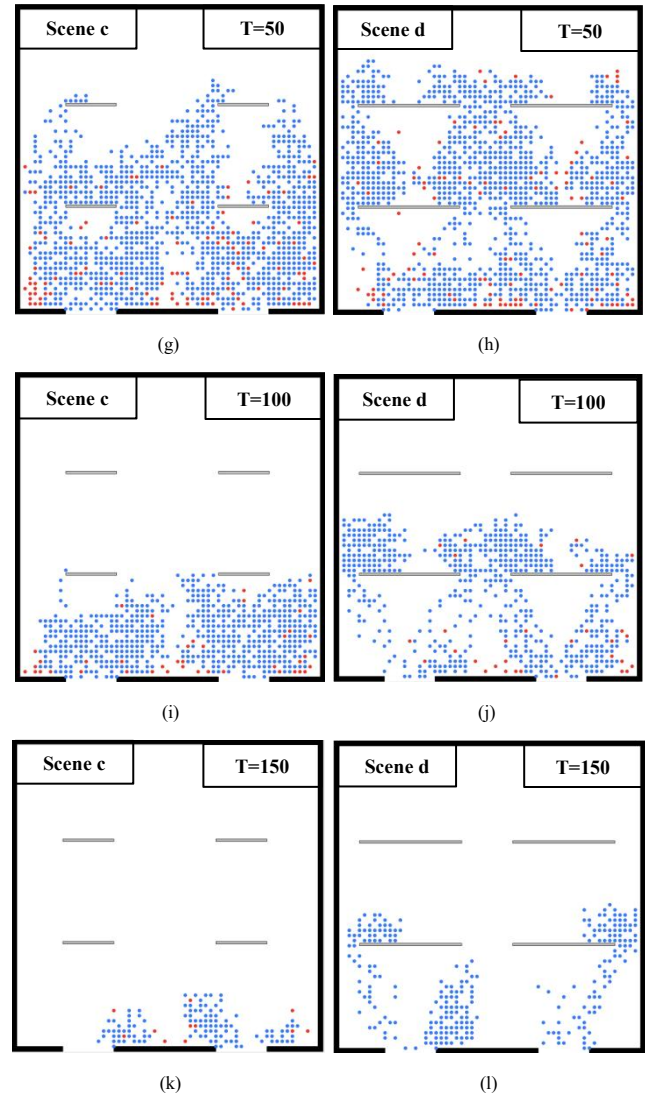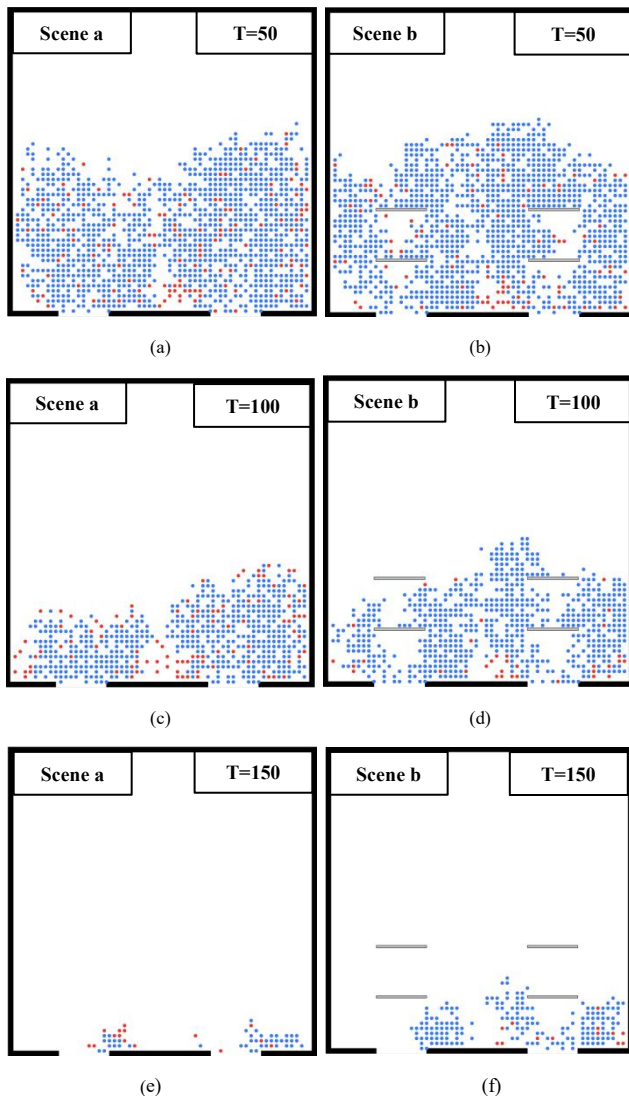

FIGURE 10. Distribution of pedestrians in 4 scenes when $r = 0.5$ and $p_{run} = 0.1$.

Obstacles in scenario b are close to the exits, and some pedestrians slow down owing to the obstacles. Most running pedestrians had enough space to move forward, benefitting from the cushioning of obstacles; thus, most of the running pedestrians approached the exit by time step 100 (see Figure 10 (d)). The speed advantage of running pedestrians is evident in the later stages of evacuation. The obstacles in Scenario c were far from the exit, which had a buffering effect on pedestrians far from the exit. Although most pedestrians bypass the obstacles and quickly gather near the exit and form aggregates and congestions, the evacuation speed is very fast compared with Scenario b. By time step 50, most pedestrians have successfully evacuated, as shown in Figure 10 (g). However, owing to the high density of pedestrians near the exit at the final stage, a small number of running pedestrians did not complete the evacuation in advance. The obstacles in scene d clearly

divide the pedestrians into three areas. The free triangle space in front of the obstacles were larger; therefore, the pedestrians showed a banding formation. The congestion in the middle area is larger and the congestion duration is longer, but the speed advantage of running pedestrians is obvious. At time step 150, all running pedestrians were evacuated, but some walking pedestrians were congested in the middle area (Figure 10 (l)). In general, when the initial pedestrian density is fixed, except when it is very close to the exit, shorter obstacles have little impact on pedestrian evacuation. The longer the obstacle, the slower is the evacuation. In a scene with obstacles, a smaller proportion of running pedestrians and shorter obstacles are profitable for evacuation.
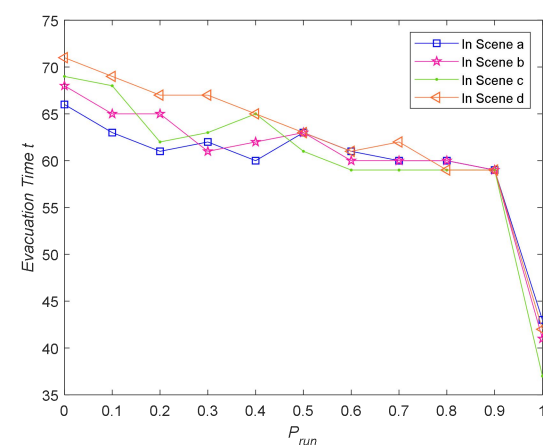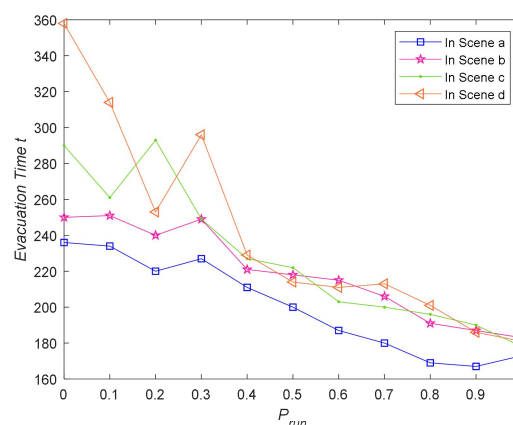

(c) $r = 0.5$

(a) $r = 0.1$
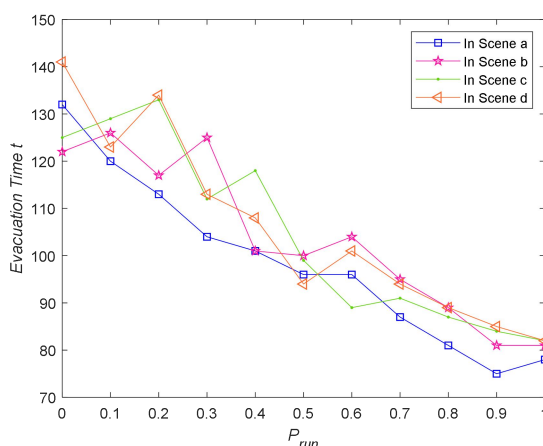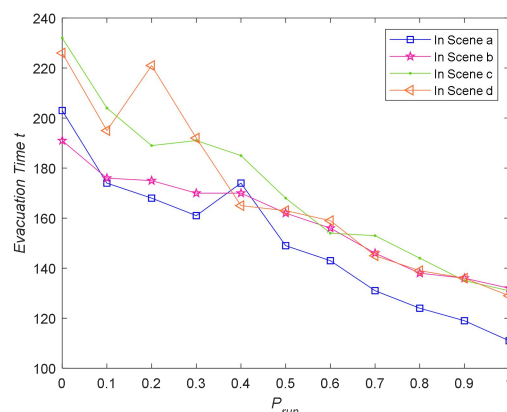
(d) $r = 0.7$

FIGURE 11. Comparison of effects of obstacle layouts on evacuation.

Figure 11 displays the comparison plots of evacuation time change with an increment of the proportion of running pedestrians. In general, the evacuation time decreased with the increase of P_{run}, indicating that the presence of running pedestrians in a crowd can improve the efficiency of evacuation. When the pedestrian density was low, the location of obstacles had no obvious effect on the evacuation time. As the proportion of running pedestrians increased, evacuation time decreased rapidly.

When the pedestrian density is fixed, the influence of the length and layouts of obstacles on evacuation is different: when the widths of obstacles and exits were same and the obstacles were evenly distributed in the place, the evacuation is fast; when the obstacles are distributed close to exits, the evacuation time is longer. When the width of the obstacle was twice the exit width, the evacuation time increases significantly. With an increase in pedestrian density in the scene, the evacuation time fluctuates significantly. This indicates that when the total number of pedestrians in the scene is large, most of the space is occupied by walking pedestrians, while the space of

(b) $r = 0.3$

running pedestrians is insufficient, then the influence of a small number of running pedestrians on evacuation is not obvious. An increase in the proportion of running pedestrians improves their evacuation efficiency.

IV. DISCUSSION

A. THE IMPACT OF THE PROPORTION OF RUNNING PEDESTRIANS ON EVACUATION

Walking and running pedestrians evacuate in the scene simultaneously, and running pedestrians may not always evacuate first. The proportion of pedestrians and the layout of facilities in the scene will have an impact on evacuation. To study the speed advantage effect of running pedestrians and ignore the influence of emotions, this study compares the evacuation time differences between walking and running pedestrians in the same scene, with and without obstacles, as well as the speed advantage of running pedestrians. We assume that the initial total number of people is fixed as $r = 0.1$, which is 360. The proportion of running pedestrians increases from 0.1 to 0.9 at intervals of 0.1. Perform mixed pedestrian evacuation in scene a and b. As shown in Figure 12, for running pedestrians, the evacuation time was significantly faster than that of walking pedestrians, especially in scene a, and the evacuation time of running pedestrians was within 60 time steps. If $r = 0.5$, the evacuation times for all pedestrians in scene a were basically the same. When the proportion of running pedestrians is higher than 0.4, the evacuation time of running pedestrians decreases significantly and rapidly with an increase in the proportion of running pedestrians. When the proportion of running pedestrians was 0.9, the evacuation time was the shortest, which was the same as the evacuation time for the same proportion of pedestrians without obstacles. This indicates that, when the total number of pedestrians is small, obstacles closer to the exit have no significant impact on pedestrian evacuation.
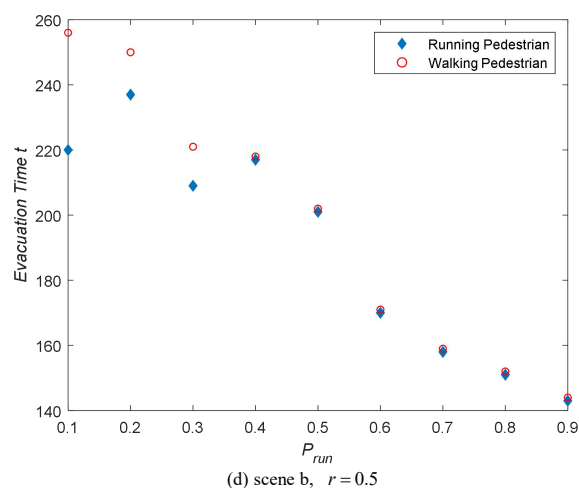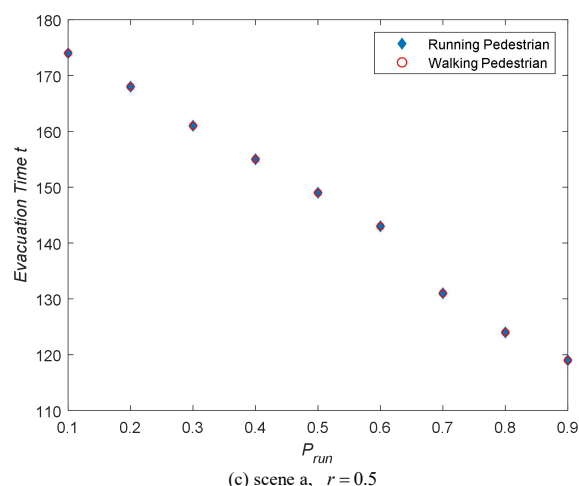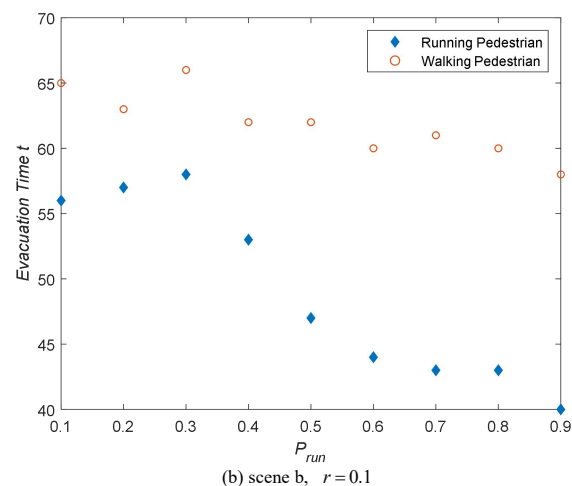

(a) scene a, $r = 0.1$

(b) scene b, $r = 0.1$

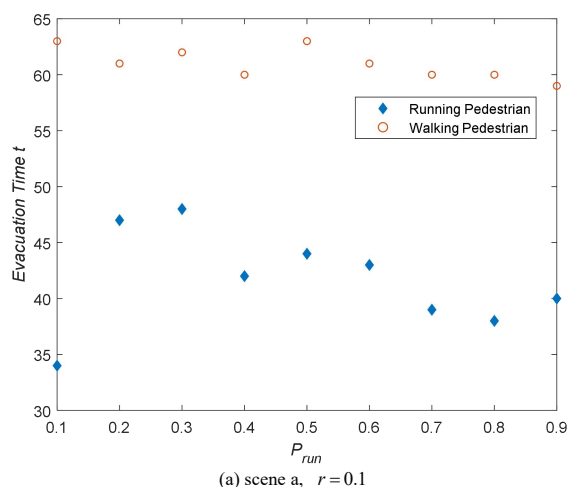(c) scene a, $r = 0.5$

(d) scene b, $r = 0.5$

FIGURE 12. Comparison of evacuation time between walking and running pedestrians.

B. UNCERTAINTY IN THE IMPACT OF OBSTACLES NEAR THE EXIT

Many researchers emphasized that placing obstacles near exits can affect evacuation efficiency. The results of

experiments in [18], [19], [20], [21], [22] indicate that placing obstacles of different shapes and sizes at different locations near exits can have a positive or negative impact on evacuation. Although there is a general consensus that obstacles can enhance the flow rate of pedestrians near an exit, there is still much uncertainty regarding the particular situations in which a column's advantages can be realized. For instance, Helbing et al. (2005) discovered that an asymmetric column positioned near an exit effectively disrupted temporarily "frozen" crowd formations, thus enabling swift evacuation during panic situations. However, in the absence of competitive behavior during normal egress, the flow rates for areas with and without columns tend to be similar. Helbing et al. [19] conducted experiments to determine the effects of obstacles on congested populations. Placing a barrier near the exit as an obstacle increased the outflow of participants by 30%, and the experimental results of Jiang et al.[20] suggested that the placement of two obstacles near the exit yielded greater effectiveness compared to the placement of just one. The experiment conducted by Liu et al.[21] tested two exit positions: one in the middle of the wall and the other in the corner. A column with a diameter of $1m$ is placed $1m$ in front of the $1.2m$ wide exit. The results indicate that placing obstacles near the exit increases pedestrian evacuation time compared to when there are no obstacles, and the pedestrian evacuation efficiency is the highest when the exit is set in the corner. Shi et al. [22] examined the influence of obstacle size and distance from the obstacle to the exit on the process of evacuation and found that the pedestrian outflow efficiency was 22.1% higher when an $0.6m$ diameter obstacle was placed $1m$ away from the middle exit compared to the distance of $0.6m$. Through simulation, Frank et al. [23] found that when the distance from the obstacle to the exit was twice the width of the exit, the pedestrian outflow increased compared to the unobstructed situation. However, as the distance increased to more than twice the width of the exit, the obstacles had no effect on the evacuation time.

For ethical and safety reasons, bottleneck experiments involving humans have been limited to non-panic situations. To avoid the lack of experimental data under panic conditions, scholars have conducted many non-human experiments to verify the impact of obstacles near exits on evacuation, but the scope of most experiments was not enough. This study attempted to simulate the impact of obstacles near exits on the evacuation time during evacuation in large enclosed spaces. As shown in Figure 13, compared to Scene a, the length of the obstacle in Scene e is $4m$, equal to the width of the exit, the distance to the exit is $1.2m$, the width of the obstacle in scenarios f and g

is $2m$, and the distance to the exit is $1.2m$. The obstacle in Scene f was located in the middle of the exit, whereas in Scene g, the obstacle was on the right side of the exit. The widths of the obstacles in Scenes h and i are $4m$ and $2m$, respectively, and the distance from the obstacle to the exit is $\sqrt{3}/2$ times the width of the exit.
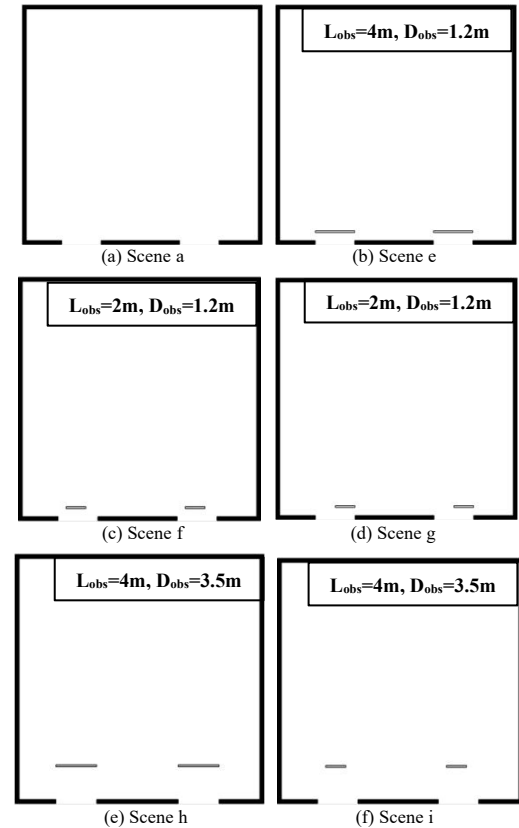

FIGURE 13. Different obstacle layouts near exits.

The relation of the pedestrian evacuation time change with the increment of the initial pedestrian proportion in these six scenarios is shown in Figure 14. The pedestrian evacuation time increased with an increase of the initial pedestrian number, and the evacuation rate in Scenario a was the fastest. When $r = 0.9$, the evacuation time was less than 300 time steps. The biggest evacuation time was more than 700 time steps in scene e (Fig. 13 (b)). When the width of the obstacle was half of the width of the exit, the evacuation time was slower than that in scene a in which there was no obstacles. When the pedestrian ratio was 0.9, the evacuation time reached 400 time-steps. However, the change of the position of the obstacle had little impact on the evacuation time. In cases where the obstacle was positioned in the middle and in the right portions of the exit (Fig. 13 (c) and (d)), the times for evacuation basically consistent. Furthermore, when the distance between the obstacle and the exit spanned $\sqrt{3}/2$ times the width of the exit (Fig. 13 (e) and (f)), variations in evacuation time due to differences in obstacle width were slight.

IEEE Access
Multidisciplinary : Rapid Review : Open Access Journal

In general, the appearance of obstacles next to the exit did not improve the evacuation efficiency. The scene area, the exit width and number of pedestrians in this study were relatively large. The farthest distance from the obstacle to the exit was $8.7m$, the nearest in $1.2m$, and the shortest width of the obstacle was $2m$. After the pedestrian passes the obstacle, a clear free triangular area is formed between the obstacle and exit. As the initial number of passengers increases, the wider the obstacle and closer it is to the exit, the more obvious the congestion is.
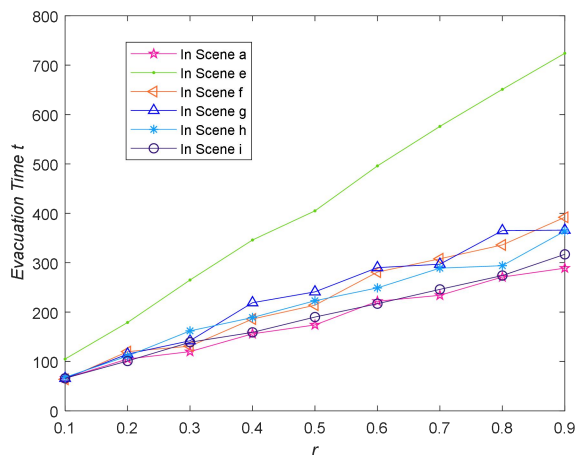

FIGURE 14. Comparison of evacuation time when obstacles are placed at different locations near exits.

V. CONCLUSIONS

To study the behavioral characteristics of individual pedestrians in depth, this paper proposed an extended cellular automata model based on dynamic potential to investigate the evacuation of walking and running pedestrians in multiple exits areas. A new update rule called "pedestrian conversion" is proposed to address the acceleration phenomenon of pedestrian in emergencies, and reflect the behaviors such as overtaking, and obstacle crossing that pedestrians exhibit during panic. The dynamic potential reflects the multiple influences of factors, such as route distance, pedestrian congestion, and route capacity[24]. Unlike the methods used in previous studies, this study considers a speed difference greater than or equal to $1m/s$ between walking and running pedestrians, with a maximum speed that can better aligns with real-world scenarios. A panic transmission mechanism was defined, namely the threshold at which walking pedestrians converted into running pedestrians. The proportion of pedestrian converted caused by panic and its impact on evacuation efficiency were analyzed.

Simulation results indicate that including a certain proportion of running pedestrians can improve evacuation efficiency. The threshold for pedestrian conversion was

adjusted according to scene type and pedestrian visibility range. The introduction of panic emotion transmission and pedestrian conversion enhanced the applicability of the model to various scenarios and better reproduced the individual behavioral characteristics of pedestrians. The widths of obstacle can led negative affect on evacuation efficiency. However, obstacles can play a buffering role by delaying congestion near the exit and enhancing pedestrian safety in large scale evacuation, but they do not improve evacuation efficiency. Theoretically, the impact of obstacles on pedestrian evacuation safety is positive. Through numerical simulations, it was found that an appropriate proportion of running pedestrians helps improve evacuation efficiency. When the total number of people is constant, the proportion of running pedestrians has little effect on the overall evacuation time, especially when the pedestrian population is large, because running pedestrians do not have a speed advantage. Acceleration requires space, and there is virtually no possibility of acceleration with a large number of pedestrians. The effect of obstacle layouts near an exit on evacuation efficiency is uncertain. In small areas or scenarios with a small number of pedestrians, placing obstacles near the exit had a noticeable impact on evacuation. However, in larger areas with a large number of pedestrians, placing obstacles near the exit does not increase the flow rate or evacuation efficiencies.

The model proposed in this article is suitable for large-scale mixed crowd evacuation and can be extended to more scenarios of pedestrians with different speeds. There are limitations to describing the behavioral characteristics of pedestrians in panic situations. In order to more accurately describe pedestrian characteristics, more differentiated emotional parameters can be added. Further research can focus on utilizing guiding signs to enhance the positive effects of obstacles.

REFERENCES

[1]M. Haghani, "Empirical methods in pedestrian, crowd and evacuation dynamics: Part I. Experimental methods and emerging topics," *Saf. Sci.*, vol. 129, Sep., 2020, Art. no. 104743.
[2] M. Haghani, "Empirical methods in pedestrian, crowd and evacuation dynamics: Part II. Field methods and controversial topics," *Saf. Sci.*, vol. 129, Sep., 2020, Art. no. 104760.
[3] P. Salamati and V. Rahimi-Movaghar, "Hajj stampede in Mina, 2015: need for intervention," *Arch. Trauma Res.*, vol. 5, no. 2, Jun. 2016, Art. no. 36308.
[4] X. Zhou, J. Hu, X. Ji, and X. Xiao, "Cellular automaton simulation of pedestrian flow considering vision and multi-velocity," *Physica A*, vol. 514, no. 15, pp. 982-992, Jan. 2019.
[5] A. Kirchner, H. Klüpfel, K. Nishinari, A. Schadschneider and M. Schreckenberg, "Discretization effects and the influence of walking speed in cellular automata models for pedestrian dynamics," *J. Stat. Mech: Theory Exp.*, p. 10011, Oct. 2004.
[6] W. Weng, L. Pan, S. Shen and H. Yuan, "Small-grid analysis of discrete model for evacuation from a hall," *Physica A*, vol. 374, no. 2, pp. 821-826,

Feb. 2007.

[7] Y. Weifeng, T.K. Hai, "A novel algorithm of simulating multi-velocity evacuation based on cellular automata modeling and tenability condition," *Physica A*, vol. 379, no. 1, pp. 250-262, Jun. 2007.

[8] R.-Y. Guo, H.-J. Huang and S. Wong, "Collection, spillback, and dissipation in pedestrian evacuation: A network-based method, " *Transport. Res. B-Meth*, vol. 45, no. 3, pp. 490-506, Mar. 2011.

[9] R.-Y. Guo, H.-J. Huang and S. Wong, "A potential field approach to the modeling of route choice in pedestrian evacuation, " *J. Stat. Mech.*, vol. 2013, p. 02010, Feb. 2013.

[10] Y. Xu and H.-J. Huang, "Simulation of exit choosing in pedestrian evacuation with consideration of the direction visual field," *Physica A*, vol. 391, no. 4, pp. 991-1000, Feb. 2012.

[11] L. Van Minh, C. Adam, R. Canal, B. Gaudou, H. Tuong Vinh, P. Taillandier, "Simulation of the emotion dynamics in a group of agents in an evacuation situation," *in Proc. Principles and Practice of Multi-Agent Systems: 13th International Conference,(PRIMA 2010)*, Kolkata, India, Nov. 12-15, 2010, pp. 604-619.

[12] H. Zhao, J. Jiang, R. Xu and Y. Ye, "SIRS model of passengers' panic propagation under self-organization circumstance in the subway emergency," *Math. Probl. Eng.*, vol. 2014, May 2014, Art. no. 608315.

[13] F.E. Cornes, G.A. Frank and C.O. Dorso, "Fear propagation and the evacuation dynamics," *Simul. Model. Pract. Th.*, vol. 95, pp. 112-133, Sep. 2019.

[14] L. Fu, W. Song, W. Lv, X. Liu and S. Lo, "Multi-grid simulation of counter flow pedestrian dynamics with emotion propagation, " *Simul. Model. Pract. Th.*, vol. 60, pp. 1-14, Jan. 2016.

[15] J. Ma, W.-g. Song, J. Zhang, S.-m. Lo and G.-x. Liao, "k-Nearest-Neighbor interaction induced self-organized pedestrian counter flow," *Physica A*, vol. 389, no. 10, pp. 2101-2117, May 2010.

[16] R.-Y. Guo, H.-J. Huang and S. Wong, "Route choice in pedestrian evacuation under conditions of good and zero visibility: Experimental and simulation results," *Transport. Res. B-Meth*, vol. 46, no. 6, pp. 669-686, Jul. 2012.

[17] X. Ren, J. Zhang and W. Song, "Flows of walking and running pedestrians in a corridor through exits of different widths," *Saf. Sci.*, vol. 133, Jan. 2021, Art. no. 105040.

[18] N. Shiwakoti and M. Sarvi, "Enhancing the panic escape of crowd through architectural design," *Transport. Res. C-Emer,*, vol. 37, pp. 260-267, Dec. 2013.

[19] D. Helbing, L. Buzna, A. Johansson and T. Werner, "Self-organized pedestrian crowd dynamics: Experiments, simulations, and design solutions," *Transport. Sci.*, vol. 39, no. 1, pp. 1-24, 2005.

[20] L. Jiang, J. Li, C. Shen, S. Yang and Z. Han, "Obstacle Optimization for Panic Flow - Reducing the Tangential Momentum Increases the Escape Speed," *PLoS ONE*, vol. 9, Art. No. 115463, Dec. 2014.

[21] Y. Liu, X. Shi, Z. Ye, N. Shiwakoti and J. Lin, "Controlled Experiments to Examine Different Exit Designs on Crowd Evacuation Dynamics," *CICTP 2016*, pp. 779-790, Jun. 2016.

[22] X. Shi, Z. Ye, N. Shiwakoti, D. Tang and J. Lin, "Examining effect of architectural adjustment on pedestrian crowd flow at bottleneck," *Physica A*, vol. 522, pp. 350-364, May 2019.

[23] G.A. Frank and C.O. Dorso, "Room evacuation in the presence of an obstacle," *Physica A*, vol. 390, no. 11, pp. 2135-2145, Jun. 2011.

[24] H.-H. Xu and R.-Y. Guo, "Simulation of bi-directional pedestrian flow by using a cell transmission model," *Simul. Model. Pract. Th.*, vol. 87 , pp. 1-14, Sep. 2018.
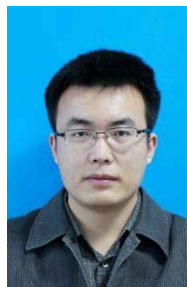
Haidong Yang   is currently pursuing the Ph.D. degree with the College of Computer Science from Inner Mongolia University. His research interests include computer vision, pedestrian traffic.

Tao Yu was born in Tongliao, Inner Mongolia, China, in 1983. She is currently pursuing the Ph.D. degree with the College of Computer Science from Inner Mongolia University. Her research interests include modeling of complex systems and simulating pedestrians and crowd dynamics .